International Journal of Experimental Design and Process Optimisation,
Volume 7, Issue 1, June 2023, pp. 62-75
DOI:10.1504/IJEDPO.2022.131230

An experimental study of laser cutting of PLA-Wood flour 3D printed plates using a modified Taguchi design

John D. Kechagias*

Forestry, Wood Science and Design Department, University of Thessaly, Karditsa, 43100, GR
E-mail: jkechag@uth.gr
* Corresponding Author

Konstantinos Ninikas

Forestry, Wood Science and Design Department, University of Thessaly, Karditsa, 43100, GR
E-mail: kninikas@uth.gr

Konstantinos Salonitis

Sustainable Manufacturing Systems Centre, Cranfield University, Bedfordshire MK43 0AL, UK
E-mail: k.salonitis@cranfield.ac.uk

Abstract: Wooden powder flour blended with thermoplastic polylactic acid (WPLA) is an eco-friendly composite material used in filament material extrusion (MEX) additive manufacturing (AM). This work investigates the effect of CO_2 laser cutting (LC) of filament MEX WPLA thin plates with variable cutting parameters on mean kerf width (Wm) and means surface roughness (Ra). The experimental design consists of three parameters with three levels each, i.e., the beam cutting direction (CD: 0, 45, 90º), the cutting speed (CS: 8, 13, 18 mm/s), and the beam power (BP: 82.5, 90, 97.5 W). Eleven experiments were performed following the Taguchi L9 orthogonal array plus two in the central point. Finally, additional combinations were run and validated the suggested modified Taguchi design resulting in acceptable mean average percentage errors (MAPE). The optimum parameters' values combination (90º CD, 18mm/s CS and 97.5W BP) results in about 8.44 μm Ra and 0.355mm Wm.

Keywords: Laser; cutting; material; extrusion; FFF; FDM; 3D-printing; Taguchi; surface response; optimisation; kerf width; roughness;

Reference to this paper should be made as follows: J.D. Kechagias, K. Ninikas and K. Salonitis. (2022) 'An experimental study of laser cutting of PLA-Wood flour 3D printed plates using a modified Taguchi design', *Int. J. Experimental Design and Process Optimisation*,

Biographical notes:

John D. Kechagias graduated from the University of Patras in 1995 with a diploma in Mechanical Engineering. He received a PhD diploma from the same University (2001) for research in laminated object manufacturing (LOM)

process optimisation and modelling. Then, he was employed on several research projects funded by the European Union at the University of Patras, and he joined TEI Thessaly in October 2004 in the Mechanical Engineering Department. In October 2020, he moved to the Department of Forestry Wood Sciences & Design at the University of Thessaly, where he is the Director of the Design and Manufacturing Laboratory. He has published numerous articles in experimental design, quality engineering, and optimisation, focusing on robust design applied in materials and manufacturing processes.

Konstantinos Ninikas holds a BEng (in Mechanical Engineering), an M.Sc. (Energy potentials from waste) and a PhD (Renewable Heat Energy from waste) from Glasgow Caledonian University, U.K. He worked at the TEI of Thessaly, and since 2019 he has been working at the Department of Forestry Wood Sciences & Design, University of Thessaly, Greece. In addition, he trained at MIT in the field of "Energy, Sustainability and Product Life Cycle" and at Harvard University in "Strategy and Innovation". He also works as a part-time lecturer at the Glasgow Caledonian University, U.K., at the School of Computing, Engineering and the Built Environment. He has also been engaged with several international research projects working with teams from different disciplines.

Konstantinos Salonitis graduated from the University of Patras with a Diploma in Mechanical Engineering in 2001 and was awarded a PhD in Manufacturing Processes in 2006. He joined Cranfield University in February 2012. He was appointed a Professor of Manufacturing Systems in October 2019. Kostas has published over 250 research papers in major international journals and internationally referred conferences and authored two books. He has supervised more than 20 PhD students to completion. He is the Head of the Sustainable Manufacturing Systems Centre at Cranfield University and has acted as a co-investigator in several projects.

1 Introduction

Laser processing of thin plates is a thermomechanical process that can achieve high process efficiency in terms of dimensional accuracy and surface quality (see Yilbas, 1998). Laser beam versatility makes drilling, cutting, welding, and etching feasible (see Steen, 2003). Laser cutting is involved in a plethora of sheet form materials such as metals (see Sudha et al., 2010), thermoplastics (see Chryssolouris, 2013), composites (see Mahrle & Beyer, 2009), and 3D printed materials (Kechagias et al., 2021). Parameter process control during laser cutting (LC) is applied at a very early stage to improve the quality of the machined surface attributes kerf geometry and surface quality (see Madić et al., 2020).

Laser processing performance is affected by various parameters. E.g., (i) the laser beam power, the continuous or pulse TEM mode, the wavelength and the beam diameter at the focal distance (see Al-Sulaiman et al., 2006); (ii) the laser beam speed, the stand-off distance, the tip (orifice) diameter, the pressure of the assist gas and the spot radius at the upper processing surface (see Choudhury & Shirley, 2010); (iii) the plate material properties such as absorptivity, upper surface texture, thickness, and thermomechanical properties (see Yue & Lau, 1996), and finally (iv) the machine parameters, including the moving mechanisms, belts, orifice weight and type, etc. (see Ninikas et al., 2021; Atanasov

& Baeva, 1997). The mean kerf width (Wm) and the mean surface roughness (Ra) are two of the most frequently investigated lasers' cutting performances (see Elsheikh et al., 2020).

Material Extrusion 3D printing, also known as Fused Filament Fabrication (FFF), is the most widespread filament MEX technology for the fabrication of final components and prototypes (see Doicin et al., 2021). However, in literature, filament MEX parts present some shape accuracy and surface quality issues that need improvement (see Kechagias et al., 2022a). E.g., dimensional characteristics deformations are shown in pins, holes, pillows and small details and are of utmost interest for improving quality 3D printings with the MEX process; see Volpato et al. (2014). Hence, post-processing methods that combine the filament MEX geometry flexibility and shape precision of the material subtraction methodologies are studied in the literature for improving the quality metrics. Therefore, hybrid laser processing with MEX technology can be assessed as an alternative to manufacturing high-precision components.

WPLA composite thermoplastic materials in different combinations of wood powders and polylactic acid are available nowadays for various applications; see Ayrilmis et al. (2019). Furthermore, the WPLA composite thermoplastics are environmentally friendly and have a wooden appearance (see Ecker et al., 2019). Zandi et al. (2020) employed an L27 Taguchi experimental design with four parameters with three levels each, i.e., the layer height (0.2, 0.3 and 0.4mm), nozzle diameter (0.5, 0.6, 0.7mm), infill density (25, 50, 75 wt.%), and printing velocity (25, 30, 35mm/s) to optimise the durability of the WPLA filament MEX parts. They proved that layer height was the most influential variable. Guessasma et al. (2019) studied, using experimental design, the impact of the printing temperature (210, 220, 230, 240, and 250 ^{o}C) on engineering stress and proved that by increasing the temperature, the ultimate tensile strength increased. However, above the 230^{o}C, the wood flour properties are reduced, i.e., degradation occurred and was not suggested. Chaidas and Kechagias (2022) proved the importance of layer thickness (0.1, 0.2, and 0.3mm) and nozzle temperature (180, 190, 200, 210, and 220^{o}C) on dimensional accuracy, surface roughness (Ra) and strength of a WPLA (30wt.%) thin-walled cube-shape (XxYxZ:20x23x30; 2mm wall thickness) specimen by using full factorial experimental design. They found that layer height affects the Ra values in the Z-direction of thin walls the most, resulting in a 18μm average, while both layer height and nozzle temperature affect the dimensional accuracy resulting in about 0.47mm error in the studied thin-walled specimens X and Y, dimensions.

Therefore, improving the 3D printed parts' dimensional accuracy and surface roughness is of high interest for better assembly quality in manufacturing products. Here, low-cost CO_2 laser cutting has been proved as an alternative for quality improvement of the fused filament fabrication 3D printing parts.

Moradi et al. (2020) utilized a continuous-wave low-power CO_2 laser to post-process PLA-FDM plates of 3.2 mm and investigated focal distance, the beam power, and the cutting beam velocity effects on the kerf geometry. They used the central composite experimental design consisting of seventeen experiments with three parameters, five levels each and second-order mathematical models to optimise kerf width. As a result, a beam velocity of 1.19 mm/s, laser power of 36.49 W, and a focal plane of 0.53 mm optimise the kerf width (276.9 μm upper and 261.5 μm down).

Kechagias et al. (2021) tested with filament material extrusion thin plates and laser beam processing cutting. PLA squared plates fabricated by filament MEX technology manufactured and then cut by a low-cost continuous-wave CO_2 Laser. They proved that

the parallel and vertical dimensions had different mean and spread values for the cut plates' kerf angle and surface roughness. They used a full factorial experimental design with three repetitions. Laser speed was between 8 and 18 mm/s, and beam power was between 82.5 and 97.5 W and achieved kerf angles lower than 1.6 degrees and Ra up to 6.2 μm.

Besides, second-order designs with the Taguchi orthogonal experimental arrays were adopted by many researchers in the laser cutting process optimisation cases. For example, Shrivastava & Pandey (2018) used the L27 Taguchi orthogonal array and second-order response methodology to optimise the laser cutting of Inconel-718. They adopted an experimental design with four parameters, three levels, and twenty-seven experiments.

There are numerous manuscripts concerning the laser processing of thin thermoplastic materials (see Hu & Zhu, 2018; Mushtaq et al., 2020; Ninikas et al., 2021), but very few regarding filament MEX materials (see Kechagias et al., 2022b; Moradi et al., 2020). Hence, the filament MEX thin plates of environmentally friendly composite materials combined with laser cutting could be an alternative for MEX components and assemblies.

Last but not least, this work proposes a modified Taguchi approach that consists of nine experiments that follow the L9 Taguchi orthogonal array plus two in the center point of the cutting direction and cutting speed parameters, resulting in eleven total experimental efforts. The results analysed by main effect plots (MEP), interaction charts, analysis of variances (ANOVA) and normality tests and new independent experiments validate the proposed methodology with the mean average percentage error (MAPE index).

2 Design of experiments

Three MEX technology 4mm plates (100x20 mm) were fabricated using a Craftbot Plus 3D printer (0.4mm nozzle diameter, 200ºC nozzle temperature, 60ºC bed temperature, 100% infill density, parallel line structure, and 0.3mm layer thickness). A Bodor BCL 1325B continuous-wave CO_2 laser with a 10.6μm wavelength, air as assist gas (1bar), and a tip diameter of 2 mm was used. After an extensive survey in the related bibliography, preliminary experimental tests, and previous experience, the parameters' values are selected. The laser beam focal spot was set at 1 mm below the upper surface, and the Stand-off Distance (SoD) was at 7mm for all cuts. Figure 1 shows the experimental laser cutting work. Note here that the cutting direction (CD) is defined as the angle between the 3D printed strands (lines) and the laser speed direction (i.e., in Figure 1, the cuts have a CD of 90º; vertical cuts). Additionally, in each experiment, the laser beam cuts a line of 10mm in length that parallels the laser table's Y-Axis.

Figure 1. Experimental work: laser cuts.

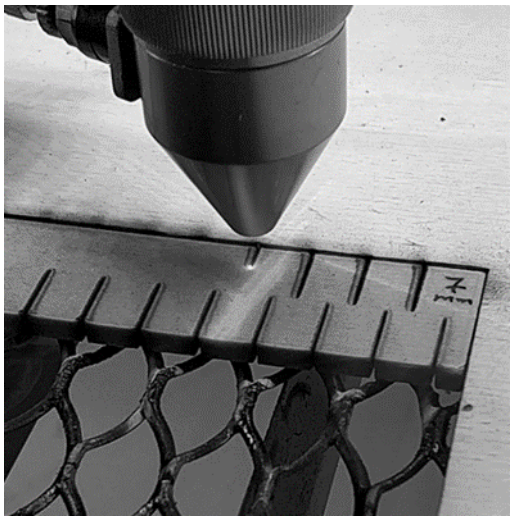

Table 1 summarizes the variable parameters and discrete levels. The laser power and cutting speed discrete values (levels) are selected carefully after the literature review (see Atanasov & Baeva, 1997) and pre-screening experiments.

Table 1. Parameters and levels.

Cutting Parameters	Abbreviation	Unit	Levels		
			1	2	3
Cutting Speed	CS	(mm/s)	8	13	18
Beam Power	BP	(W)	82.5	90.0	97.5
Cutting Direction	CD	(degrees)	0	45	90

Table 2 displays the modified Taguchi design with the eleven experiments. The first nine experiments followed the Taguchi L9 orthogonal array (three first columns used only). Then added, the tenth and eleventh central values of the cutting direction (45º) and cutting speed (13mm/s) to increase the experiment degrees of freedom.

Table 2. Modified Taguchi experimental design.

	Inputs			Outputs	
Ex. No	CD (deg.)	CS (mm/s)	BP (W)	Ra (μm)	Wm (mm)
1	0	8	82.5	9.973	0.544
2	0	13	90.0	8.760	0.481
3	0	18	97.5	6.012	0.466
4	45	8	90.0	11.451	0.690
5	45	13	97.5	9.659	0.505
6	45	18	82.5	7.909	0.403
7	90	8	97.5	11.431	0.637
8	90	13	82.5	10.311	0.515

9	90	18	90.0	8.171	0.331
10	45	13	82.5	10.723	0.573
11	45	13	90.0	10.363	0.539

A digital microscope measured the upper and down kerf widths, and then the mean Wm was calculated (Figure 2a,b). Next, the Surftest SJ-210 profilometer measured the average roughness height (Ra). The surface roughness parameters have been measured parallel to the cutting speed direction at the center of the cut surfaces; see Figure 2c, d. Note that the upper and down kerf measurements were averages of five across the 10mm cutting line.

Equation 1 calculates the mean kerf width (Wm) (See Figure 2 a,b):

$$Wm = \frac{\frac{\sum_{i=1}^{5} upper\ m_i}{5} + \frac{\sum_{i=1}^{5} bottom\ m_i}{5}}{2} \qquad (1)$$

while average surface roughness (Ra) is calculated by the following formula (see Figure 2c,d):

$$Ra = \frac{1}{l}\int_0^l |y(x)|\, dx \qquad (2)$$

Figure 2. Measurements: (a,b) Mean kerf width, and (c,d) Average surface roughness Ra.

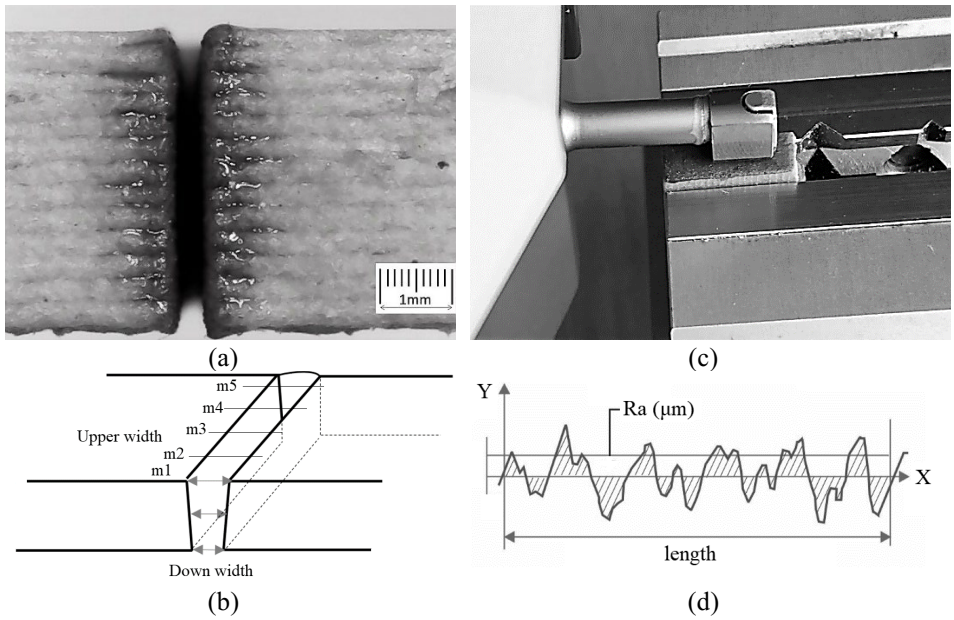

3 Results analysis

Main effect plots and interaction plots

In recent literature, the experimental results obtained using organized statistical experiments are explained by analyzing means and the analysis of variances or other statistical descriptive tools. Therefore, the main effect plots (MEP) are initially used to describe the effects of the variable parameters on outputs (Figure 3).

The cutting direction, cutting speed and laser beam power change redistribute the laser energy inside the kerf geometry, leading to complex mass and heat flow attributes of the molten material and resulting in different kerf width and surface roughness values of the cutting edges.

It is observed that the cutting direction parameter had minor effects on the mean kerf width (Wm) and significantly impacted the average surface roughness (Ra). Physically, the CD parameter does not affect energy distribution inside the kerf geometry resulting in almost the same kerf geometry for solid 3D printing material. Besides, the CD affects the Ra due to the different alignments of the filament with the cutting direction. Zero angles of the CD parameter result in better Ra values. The upsurge of the cutting speed reduces the energy distribution inside the kerf geometry resulting in lesser Wm and Ra values. At the same time, the beam power increase increases the energy distribution per unit area, resulting in higher Wm and lower Ra values.

Figure 3. MEP plots: (a) Ra, and (b) Wm

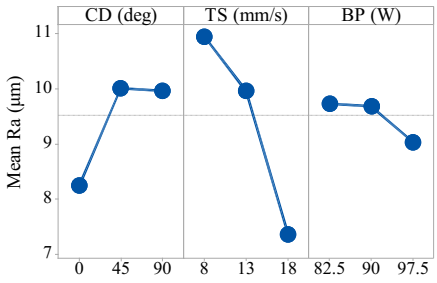

(a)

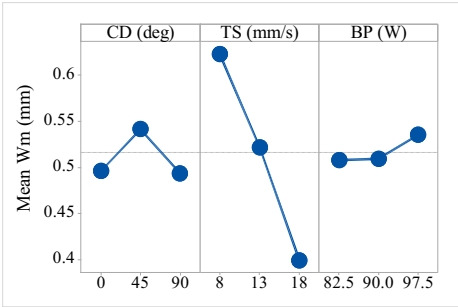

(b)

Follows the interaction charts between the variable parameters:

- Cutting speed and cutting direction interactions (Figures 4a and 4b) for the Wm and Ra show synergistic trends, while the lines are almost parallel (Ra) or in the same direction (Wm).
- Beam power and cutting direction interactions are more complicated (Figures 4c and 4d) for Wm and Ra showing significant interactions.
- Beam power and cutting speed interactions are synergistic with lines in the same directions (Figures 4e and 4f).

Figure 4. Interaction plots Ra and Wm vs.: (a, b) cutting direction and cutting speed, (c, d) cutting direction and beam power, and (e, f) cutting speed and beam power.

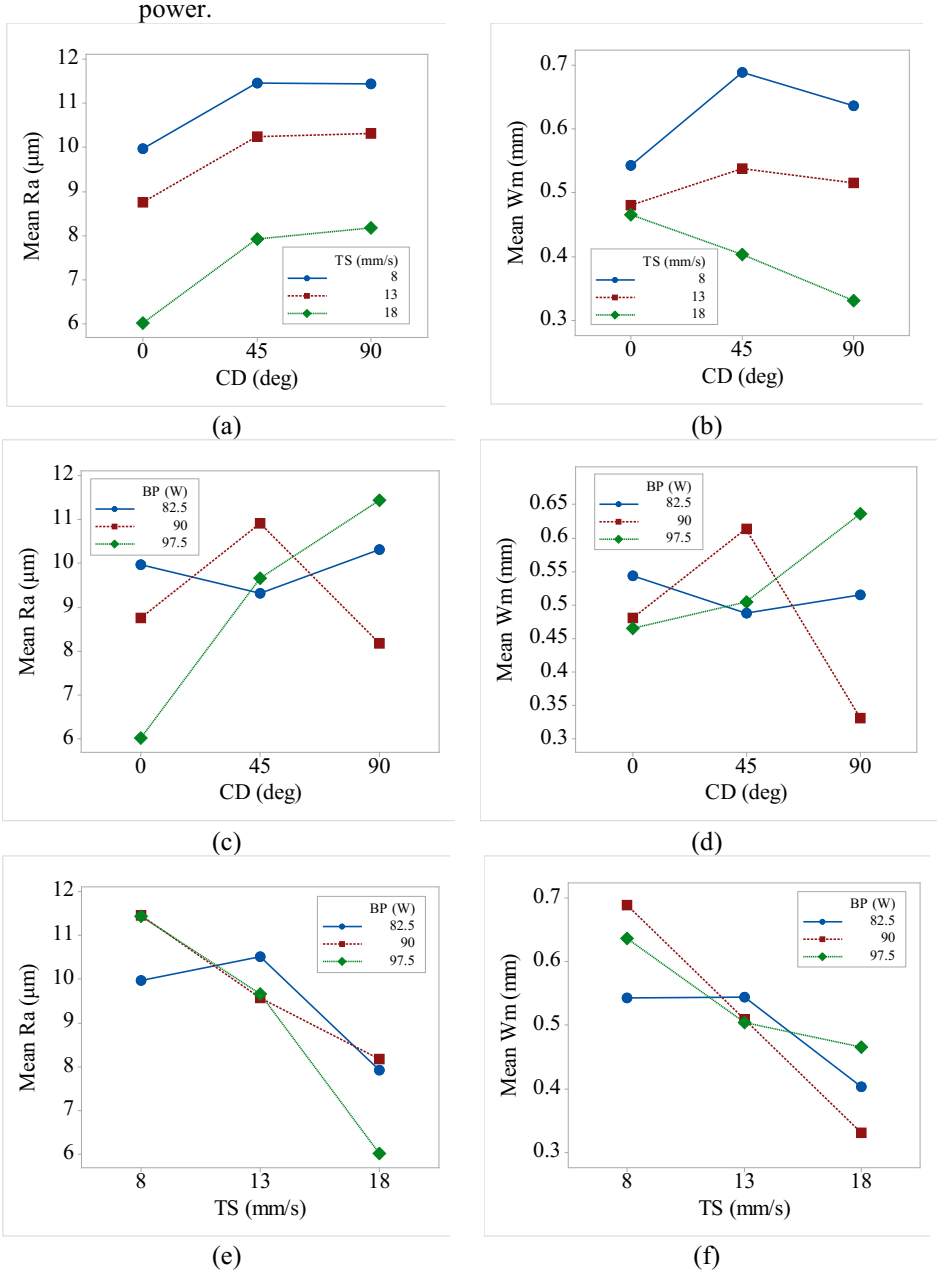

Second order approach

The full quadratic mathematical model adopted for hybrid processing optimisation in laser cutting of filament MEX WPLA thin plates; see Eq. 3. The responses (outputs; Y) here are the Wm and Ra and the variable parameters (inputs; xi) the cutting direction, cutting speed and beam power.

$$Y = b_0 + \sum_{i=1}^{n} b_i x_i + \sum_{i<j} \sum_{j} b_{ij} x_i x_j + \sum_{i=1}^{n} b_{ii} x_i^2 \pm e \qquad (3)$$

ANOVA measures the response surface methodology (RSM) performance with the variable parameters and their products (see Tables 3 and 4). The full quadratic response models fit better with the data (results) if they achieve an R-square index higher than 0.95. Also, the F value of the regression models should be higher than four (4) and p-values lower than 0.05 (null hypothesis). Here, R-sq values are higher than 0.95 and F values higher than 4, indicating good fitting of the regression model. But the p-values are higher than 0.05 (0.114 and 0.207 for Ra and Wm), which means a higher than 5% probability of observing extreme values that do not fit regression models.

Therefore, the normality test for the residuals is advised or evaluation of the model with new independent data, i.e., the MAPE index.

Table 3. ANOVA: Ra versus cutting direction; cutting speed; beam power.

Source	DoF	Adj SS	Adj MS	F-Value	P-Value
Regression	9	27.6203	3.06892	45.74	0.114
CS	1	0.0329	0.03294	0.49	0.611
CD	1	0.0363	0.03626	0.54	0.596
BP	1	0.1991	0.19905	2.97	0.335
CD*CS	1	0.1792	0.17922	2.67	0.350
CD*BP	1	0.1864	0.18638	2.78	0.344
CS*BP	1	0.1140	0.11398	1.70	0.417
CD*CD	1	1.1499	1.14989	17.14	0.151
CS*CS	1	0.8927	0.89267	13.30	0.170
BP*BP	1	0.2561	0.25607	3.82	0.301
Error	1	0.0671	0.06710		
Total	10	27.6874			
				S	0.259034
				R-sq	99.76%
				R-sq(adj)	97.58%

Table 4. ANOVA: Wm versus cutting direction; cutting speed; beam power.

Source	DoF	Adj SS	Adj MS	F-Value	P-Value
Regression	9	0.099411	0.011046	13.62	0.207
CS	1	0.002656	0.002656	3.28	0.321
CD	1	0.001485	0.001485	1.83	0.405
BP	1	0.000800	0.000800	0.99	0.502
CD*CS	1	0.006498	0.006498	8.01	0.216

CD*BP	1	0.000013	0.000013	0.02	0.921
CS*BP	1	0.001581	0.001581	1.95	0.396
CD*CD	1	0.007210	0.007210	8.89	0.206
CS*CS	1	0.000362	0.000362	0.45	0.625
BP*BP	1	0.001083	0.001083	1.34	0.454
Error	1	0.000811	0.000811		
Total	10	0.100222			
				S	0.0284753
				R-sq	99.19%
				R-sq(adj)	91.91%

ANOVA analyses show that the second-order mathematical models fit the experimental results with F-values of 45.75 and 13.62 for Ra and Wm.

The second order of CD and CS parameters are influential for Ra, having very high F values (17.14 and 13.30, respectively). For Wm, the products CD*CS and CD*CD are the most significant, having F values of 8.01 and 8.89, respectively.

The normality of the predicted output distributions should be checked, as proposed by Johnson & Montgomery (2009). Below, Figure 5 shows the normality of the errors. Here the p-values upper than 0.05 means that the distribution fits well with the normal distribution.

Figure 5. Normality plots: (a) Ra, and (b) Wm.

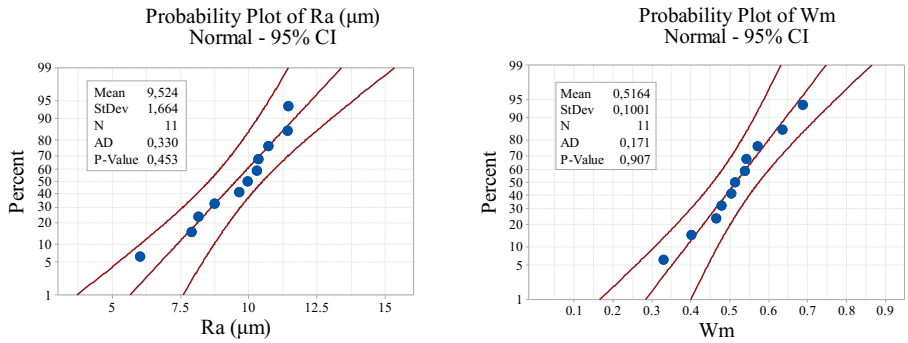

(a) (b)

The second-order surfaces for all pairs of continuous parameters are illustrated in Figures 6 and 7 for mean kerf width (Wm, mm) and average surface roughness (Ra, µm).

Figure 6. Second-order surfaces for Wm (mm) for all pairs of parameters.

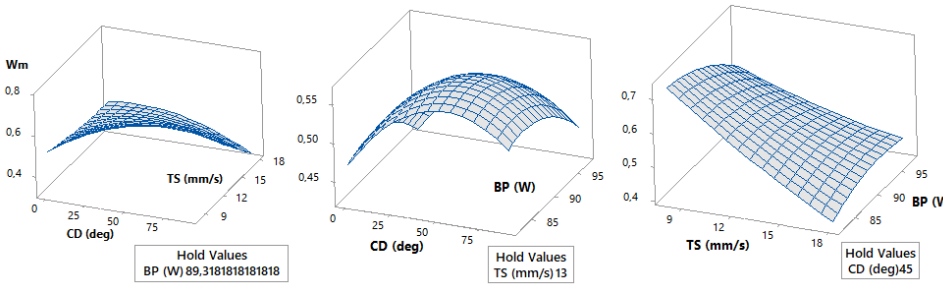

Figure 7. Second-order surfaces for Ra (µm) for all pairs of parameters.

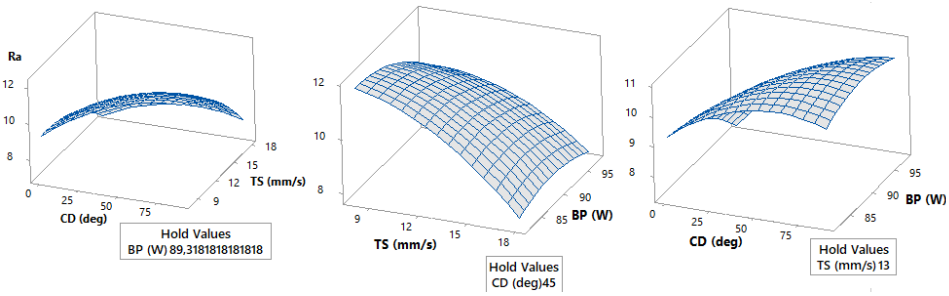

Last but not least, the extracted second-order mathematical models were used to optimise the process. Figure 8 shows the optimal parameter values for minimum Ra and Wm. The 90 degrees cutting direction, 18mm/s cutting speed and 97.5 W beam power optimise the cutting surface Ra and Wm values (0.8765µm and 0.2815mm, respectively).

Figure 8. Optimized parameter values for minimum Ra and Wm; 90ºCD, 18mm/s CS, and 82.5W BP.

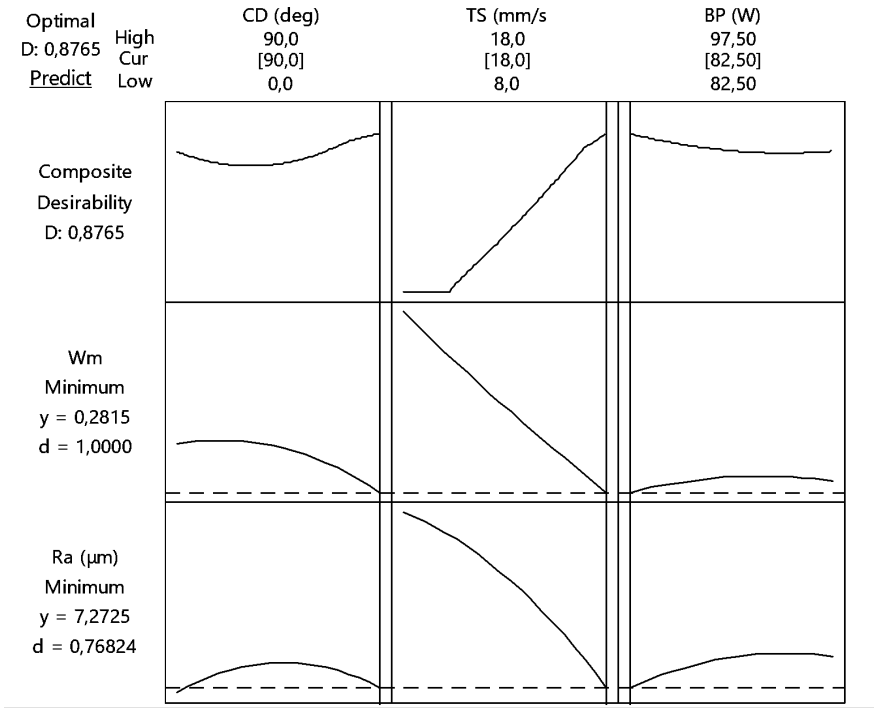

Validation

Another index that measures the performance of the response is the mean average percentage error, also known as the MAPE index (see Kechagias et al., 2022c). In Table 5, the MAPE values for the eleven experiments (Table 2) and the MAPE for the optimal conditions of process optimisation (Figure 6) are depicted. It is observed that the best combination (90ºCD, 18mm/s CS, and 82.5W BP) give very close values for the Ra and Wm. Besides, a second evaluation experiment was run at 97.5W beam power, ensuring that the mathematical models could predict the Ra and Wm suitably.

Table 5. MAPE evaluation of RSM models.

No Exp.	CD	CS	BP	Ra (μm)	Ra predict	ABS (error Ra)	Wm (mm)	Wm predict	ABS (error Wm)
1	0	8	82.5	9.97	10.03	0.5%	0.544	0.549	1.1%
2	0	13	90	8.76	8.71	0.6%	0.481	0.475	1.2%
3	0	18	97.5	6.01	6.01	0.0%	0.466	0.466	0.0%
4	45	8	90	11.45	11.40	0.5%	0.690	0.684	0.8%
5	45	13	97.5	9.66	9.66	0.0%	0.505	0.505	0.0%
6	45	18	82.5	7.91	7.96	0.7%	0.403	0.409	1.4%
7	90	8	97.5	11.43	11.43	0.0%	0.637	0.637	0.0%
8	90	13	82.5	10.31	10.36	0.5%	0.515	0.521	1.1%

9	90	18	90	8.17	8.12	0.6%	0.331	0.325	1.8%
10	45	13	82.5	10.72	10.56	1.5%	0.573	0.555	3.0%
11	45	13	90	10.36	10.52	1.5%	0.539	0.556	3.2%
					MAPE	0.6%			1.2%
Evaluation experiments									
1	90	18	82.5	8.74	7.27	16.8%	0.331	0.281	14.8%
2	90	18	97.5	8.44	8.14	3.5%	0.355	0.315	11.3%
					MAPE	10.2%			13.0%

4 Conclusions

The cutting direction, cutting speed and beam power processing parameters were studied on surface roughness and kerf width of cut surfaces during a low-power CO_2 laser cutting of WPLA MEX thin plates. It adopted a modified Taguchi experimental design and extracted the main effect plots and interaction charts for decomposing the parameter impact on mean surface roughness and kerf width. Second-order regression modes were used to fit the experimental (output) data with the processing (input) parameters and were evaluated with ANOVA, response normality plots and mean absolute percentage error (MAPE).

The MEP plots and interaction charts conclude on:

- The cutting direction is influential for the Ra cutting surfaces due to the effects of filament deposition on the cutting direction while affecting the Wm moderately.
- The cutting speed is the dominant parameter for the Ra and Wm. This is because the energy distribution inside kerf geometry decreases when cutting speed increases, affecting all the metrics.
- Finally, when the beam power increases, the energy inside the kerf geometry increases, and the Ra improves slightly while the Wm increases somewhat.

The second-order response models' ANOVA evaluation results in F values higher than 4, Rsq higher than 0.95 (Tables 3 and 4) and normality test p-values higher than 0.05 (Figure 5), indicating good fitting. The values of the optimised processing parameters were calculated using the second-order models; 90ºCD, 18mm/s CS and 97.5W BP. Additionally, the MAPE index evaluated the second-order models resulting in values lower than 2% for the modified Taguchi experiments and lower than 13% for two new experiments in optimal conditions (Table 5).
The authors propose the investigation of more filament-MEX processing parameters, such as infill density and pattern, for shape and surface MEX-parts improvement with laser processing as future work.

References

Al-Sulaiman, F. A., Yilbas, B. S., & Ahsan, M. (2006). CO2 laser cutting of a carbon/carbon multi-lamelled plain-weave structure. Journal of Materials Processing Technology, 173(3), 345–351. https://doi.org/10.1016/j.jmatprotec.2005.12.004

Atanasov, P. A., & Baeva, M. G. (1997, April 4). CW CO 2 laser cutting of plastics. XI International Symposium on Gas Flow and Chemical Lasers and High-Power Laser Conference. https://doi.org/10.1117/12.270185

Ayrilmis, N., Kariz, M., Kwon, J. H., & Kitek Kuzman, M. (2019). Effect of printing layer thickness on water absorption and mechanical properties of 3D-printed wood/PLA composite materials. The International Journal of Advanced Manufacturing Technology, 102(5–8), 2195–2200. https://doi.org/10.1007/s00170-019-03299-9

Chaidas, D., & Kechagias, J. D. (2022). An investigation of PLA/W parts quality fabricated by FFF. Materials and Manufacturing Processes, 37(5), 582–590. https://doi.org/10.1080/10426914.2021.1944193

Choudhury, I. A., & Shirley, S. (2010). Laser cutting of polymeric materials: An experimental investigation. Opt. Laser Technol., 42(3), 503–508. https://doi.org/10.1016/j.optlastec.2009.09.006

Chryssolouris, G. (2013). Laser machining: theory and practice. Springer Science & Business Media. Springer Science & Business Media.

Doicin, C. V., Ulmeanu, M. E., Rennie, A. E. W., & Lupeanu, E. (2021). Mass optimisation of 3D-printed specimens using multivariable regression analysis. International Journal of Rapid Manufacturing, 10(1), 1. https://doi.org/10.1504/IJRAPIDM.2021.119936

Ecker, J. V., Haider, A., Burzic, I., Huber, A., Eder, G., & Hild, S. (2019). Mechanical properties and water absorption behaviour of PLA and PLA/wood composites prepared by 3D printing and injection moulding. Rapid Prototyping Journal, 25(4), 672–678. https://doi.org/10.1108/RPJ-06-2018-0149

Elsheikh, A. H., Deng, W., & Showaib, E. A. (2020). Improving laser cutting quality of polymethylmethacrylate sheet: experimental investigation and optimization. Journal of Materials Research and Technology, 9(2), 1325–1339. https://doi.org/10.1016/j.jmrt.2019.11.059

Guessasma, Belhabib, & Nouri. (2019). Microstructure and Mechanical Performance of 3D Printed Wood-PLA/PHA Using Fused Deposition Modelling: Effect of Printing Temperature. Polymers, 11(11), 1778. https://doi.org/10.3390/polym11111778

Hu, J., & Zhu, D. (2018). Experimental study on the picosecond pulsed laser cutting of carbon fiber-reinforced plastics. Journal of Reinforced Plastics and Composites, 37(15), 993–1003. https://doi.org/10.1177/0731684418775807

Johnson, R. T., & Montgomery, D. C. (2009). Choice of second-order response surface designs for logistic and Poisson regression models. International Journal of Experimental Design and Process Optimisation, 1(1), 2. https://doi.org/10.1504/IJEDPO.2009.028954

Kechagias, J., Chaidas, D., Vidakis, N., Salonitis, K., & Vaxevanidis, N. M. (2022a). Key parameters controlling surface quality and dimensional accuracy: a critical review of FFF process. Materials and Manufacturing Processes, 1–22. https://doi.org/10.1080/10426914.2022.2032144

Kechagias, J., Ninikas, K., Petousis, M., & Vidakis, N. (2022b). Laser cutting of 3D printed acrylonitrile butadiene styrene plates for dimensional and surface roughness optimization. The International Journal of Advanced Manufacturing Technology, 119(3–4), 2301–2315. https://doi.org/10.1007/s00170-021-08350-2

Kechagias, J., Ninikas, K., Petousis, M., Vidakis, N., & Vaxevanidis, N. (2021). An investigation of surface quality characteristics of 3D printed PLA plates cut by CO2 laser using experimental design. Materials and Manufacturing Processes, 36(13), 1544–1553. https://doi.org/10.1080/10426914.2021.1906892

Kechagias, J., Tsiolikas, A., Petousis, M., Ninikas, K., Vidakis, N., & Tzounis, L. (2022c). A robust methodology for optimizing the topology and the learning parameters of an ANN for accurate predictions of laser-cut edges surface roughness. Simulation Modelling Practice and Theory, 114, 102414. https://doi.org/10.1016/j.simpat.2021.102414

Madić, M., Mladenović, S., Gostimirović, M., Radovanović, M., & Janković, P. (2020). Laser cutting optimization model with constraints: Maximization of material removal rate in CO2 laser cutting of mild steel. Proceedings of the Institution of Mechanical Engineers, Part B: Journal of Engineering Manufacture, 234(10), 1323–1332. https://doi.org/10.1177/0954405420911529

Mahrle, A., & Beyer, E. (2009). Theoretical aspects of fibre laser cutting. Journal of Physics D: Applied Physics, 42(17), 175507. https://doi.org/10.1088/0022-3727/42/17/175507

Moradi, M., Karami Moghadam, M., Shamsborhan, M., Bodaghi, M., & Falavandi, H. (2020). Post-Processing of FDM 3D-Printed Polylactic Acid Parts by Laser Beam Cutting. Polymers, 12(3). https://doi.org/10.3390/polym12030550

Mushtaq, R. T., Wang, Y., Rehman, M., Khan, A. M., & Mia, M. (2020). State-Of-The-Art and Trends in CO2 Laser Cutting of Polymeric Materials—A Review. Materials, 13(17). https://doi.org/10.3390/ma13173839

Ninikas, K., Kechagias, J., & Salonitis, K. (2021). The Impact of Process Parameters on Surface Roughness and Dimensional Accuracy during CO2 Laser Cutting of PMMA Thin Sheets. J. Manuf. Mater. Process., 5(3). https://doi.org/10.3390/jmmp5030074

Shrivastava, P. K., & Pandey, A. K. (2018). Geometrical quality evaluation in laser cutting of Inconel-718 sheet by using Taguchi based regression analysis and particle swarm optimization. Infrared Physics & Technology, 89, 369–380. https://doi.org/10.1016/j.infrared.2018.01.028

Steen, W. M. (2003). Laser material processing—an overview. Journal of Optics A: Pure and Applied Optics, 5(4), S3–S7. https://doi.org/10.1088/1464-4258/5/4/351

Sudha, C., Parameswaran, P., Krishnan, R., Dash, S., & Vijayalakshmi, M. (2010). Effect of Laser Shock Processing on the Microstructure of 304(L) Austenitic Stainless Steel. Materials and Manufacturing Processes, 25(9), 956–964. https://doi.org/10.1080/10426911003720763

Volpato, N., Aguiomar Foggiatto, J., & Coradini Schwarz, D. (2014). The influence of support base on FDM accuracy in Z. Rapid Prototyping Journal, 20(3), 182–191. https://doi.org/10.1108/RPJ-12-2012-0116

Yilbas, B. S. (1998). Study of Parameters for CO2 Laser Cutting Process. Materials and Manufacturing Processes, 13(4), 517–536. https://doi.org/10.1080/10426919808935273

Yue, T. M., & Lau, W. S. (1996). Pulsed Nd:YAG Laser Cutting of Al/Li/SiC Metal Matrix Composites. Materials and Manufacturing Processes, 11(1), 17–29. https://doi.org/10.1080/10426919608947458

Zandi, M. D., Jerez-Mesa, R., Lluma-Fuentes, J., Roa, J. J., & Travieso-Rodriguez, J. A. (2020). Experimental analysis of manufacturing parameters' effect on the flexural

properties of wood-PLA composite parts built through FFF. Int. J. Adv. Manuf. Technol., 106(9–10), 3985–3998. https://doi.org/10.1007/s00170-019-04907-4

2023-05-30

An experimental study of laser cutting of PLA-wood flour 3D printed plates using a modified Taguchi design

Kechagias, John D.

Inderscience

Kechagias JD, Ninikas K, Salonitis K. (2023) An experimental study of laser cutting of PLA-wood flour 3D printed plates using a modified Taguchi design. International Journal of Experimental Design and Process Optimisation, Volume 7, Issue 1, June 2023, pp. 62-75
https://doi.org/10.1504/IJEDPO.2022.131230